

Article

Blind Phase Search with Angular Quantization Noise Mitigation for Efficient Carrier Phase Recovery

Jaime Rodrigo Navarro ^{1,2,*}, Aditya Kakkar ^{1,2}, Richard Schatz ², Xiaodan Pang ²,
Oskars Ozolins ¹, Aleksejs Udalcovs ¹, Sergei Popov ² and Gunnar Jacobsen ¹

¹ Networking and Transmission Laboratory, RISE Acreo AB, SE-164 40 Kista, Sweden; adityak@kth.se (A.K.); oskars.ozolins@ri.se (O.O.); aleksejs.udalcovs@ri.se (A.U.); gunnar.jacobsen@ri.se (G.J.)

² School of Engineering Sciences, KTH Royal Institute of Technology, SE-100 44, Stockholm, Sweden; rschatz@kth.se (R.S.); xiaodan@kth.se (X.P.); sergeip@kth.se (S.P.)

* Correspondence: jaime.rodrido-navarro@ri.se; Tel.: +46-76-282-77-40

Received: 19 April 2017; Accepted: 18 May 2017; Published: 23 May 2017

Abstract: The inherent discrete phase search nature of the conventional blind phase search (C-BPS) algorithm is found to introduce angular quantization noise in its phase noise estimator. The angular quantization noise found in the C-BPS is shown to limit its achievable performance and its potential low complexity implementation. A novel filtered BPS algorithm (F-BPS) is proposed and demonstrated to mitigate this quantization noise by performing a low pass filter operation on the C-BPS phase noise estimator. The improved performance of the proposed F-BPS algorithm makes it possible to significantly reduce the number of necessary test phases to achieve the C-BPS performance, thereby allowing for a drastic reduction of its practical implementation complexity. The proposed F-BPS scheme performance is evaluated on a 28-Gbaud 16QAM and 64QAM both in simulations and experimentally. Results confirm a substantial improvement of the performance along with a significant reduction of its potential implementation complexity compared to that of the C-BPS.

Keywords: blind phase search (BPS); carrier phase estimation (CPE); carrier phase recovery (CPR); coherent detection; quadrature amplitude modulation (mQAM); phase noise

1. Introduction

Carrier phase recovery (CPR) is an essential block to estimate and compensate for the phase noise introduced by the free running lasers in coherent optical communication systems. Two approaches for CPR are conventionally employed based on either the M -th power operation [1] or on the conventional blind phase search (C-BPS) algorithm [2]. The M -th power operation approach provides a poorer phase noise tolerance for high order constellations as only a small percentage of constellation points can be employed for phase noise estimation. Additionally, the accuracy of symbol amplitude discrimination required for symbol classification or partitioning in this approach decreases for low optical to signal noise ratios (OSNRs) or high order constellations [3–5]. On the other hand, the C-BPS approach provides high phase noise tolerance at the expense of a high computational complexity. The number of required test phases to achieve high phase noise tolerance largely increases with the modulation order which increases the overall computational complexity of the algorithm and becomes a burden for its practical implementation. Alternatively, multi-stage CPR schemes employing both approaches in different stages have also been proposed with the aim of providing good phase noise tolerance while maintaining a relatively low overall computational complexity [3–12]. However, the implementation complexity reductions achieved by the proposed multi-stage algorithms are not the minimum achievable and could be further reduced by overcoming the inherent limitations of the C-BPS stage provided in this manuscript. High phase noise tolerant CPR schemes at low implementation complexity levels would make it possible to use smaller integrated DFB lasers, driven

at low power for high order modulations or DBR lasers with electronic tuning via carrier injection instead of thermal tuning.

In this paper, we demonstrate the inherent limitation of the C-BPS algorithm due to angular quantization noise and propose a cost effective solution to mitigate it, using a post-BPS low pass filter (LPF). The proposed filtered BPS (F-BPS) scheme increases the phase noise tolerance while it reduces the computational complexity compared to that of the C-BPS. The performance of the F-BPS algorithm is evaluated for 16QAM and 64QAM through simulations. Experimental validation of the F-BPS scheme on a 28-Gbaud 64QAM is also performed. Results show a noticeable enhancement in the phase noise tolerance of the proposed F-BPS scheme compared to C-BPS and an achievable drastic reduction of its computational complexity for its practical implementation.

2. Principle of the Proposed Angular Quantization Noise Filter in F-BPS

The operation principle of the proposed F-BPS scheme is illustrated in Figure 1. As in the C-BPS, a block of $2M + 1$ symbols is rotated by a number of test phases B . The resulting rotated blocks of symbols for each of the test phases are then fed into a decision circuit module where the closest constellation points in the original constellation are determined. The squared distances of $2M + 1$ symbols to its closest constellation points in the original constellation are calculated for each of the rotated block of symbols. The sum of $2M + 1$ square distances is considered for averaging the impact of additive white Gaussian noise (AWGN), which is known as the C-BPS block filter [2]. The angular rotation providing the minimum distance metric sum is considered to be the phase noise estimator for the symbol in the middle of the block. An unwrap module is then required to minimize cycle slip occurrence. The phase noise estimator after the unwrap module corresponds to the final estimator in the C-BPS algorithm ($\hat{\beta}$). It is worth noting that $\hat{\beta}$ has been selected from a set of discrete angular values. Therefore, $\hat{\beta}$ contains quantization noise and, when it is employed for phase noise compensation as in the C-BPS, results in angular quantization noise in the corrected signal.

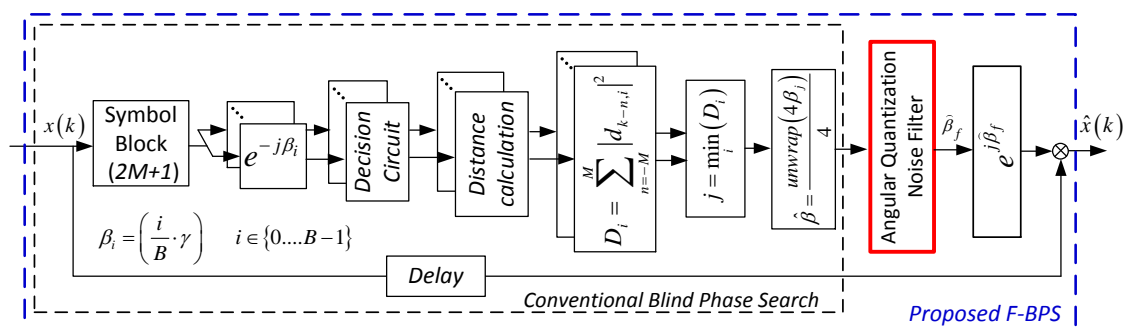


Figure 1. Block diagram of the C-BPS CPR scheme and the proposed F-BPS scheme employing the angular quantization noise filter.

Figure 2a shows the frequency noise spectrum (FN-PSD) of the phase tracked by the C-BPS algorithm ($\hat{\beta}$) for different values of test phases in a sliding window CPR approach. Increased frequency noise in the C-BPS phase estimator is observed with decreased number of test phases. This is due to the discrete phase search nature of the C-BPS algorithm, introducing quantization noise in its phase noise estimator. The first observed dip in Figure 2a (see $\beta = 64$ curve) corresponds to the C-BPS block filter bandwidth which defines the estimation bandwidth of the C-BPS. It is observed how the out-of-band frequency components increase as the number of employed test phases reduces due to angular quantization noise. Figure 2b shows the temporal quantized phase evolution tracked by the C-BPS algorithm ($\hat{\beta}$) for different numbers of test phases and a sliding window CPR approach. The discrete angular jumps due to angular quantization in the C-BPS are bigger for lower values of employed test phases which translates into larger quantization noise as illustrated correspondingly in

Figure 2a. The proposed F-BPS scheme shown in Figure 1 uses an angular quantization noise filter consisting of a low pass filter operation performed on the C-BPS phase noise estimator to mitigate its out-of-band angular quantization noise. The proposed angular quantization noise filter in the F-BPS must be designed such that it removes the out-of-band noise enhancement while preserving the in band information of the original C-BPS phase estimator contained within the C-BPS block filter bandwidth (see Figure 2a). The improved F-BPS phase noise estimator (β_f) after the proposed angular quantization noise filter is then used to compensate for the phase noise of the original signal as illustrated in Figure 1.

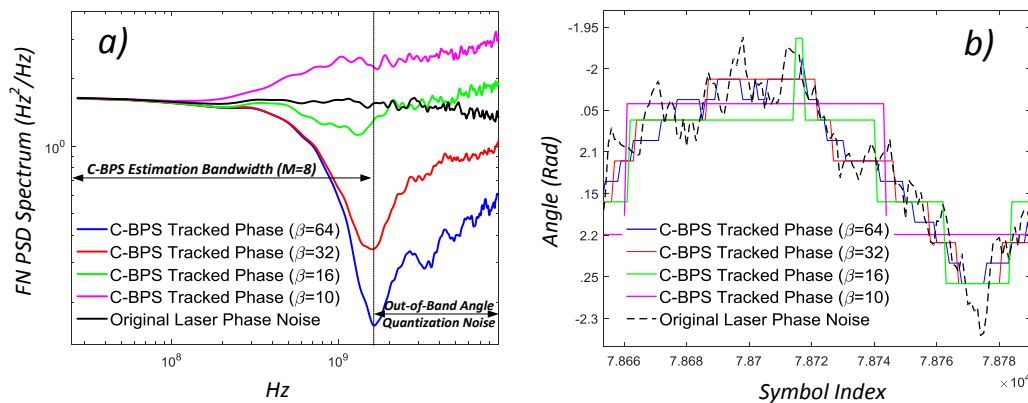


Figure 2. (a) FN-PSD of different tracked phases by the C-BPS algorithm employing different number of test phases; (b) time domain tracked phase by the C-BPS algorithm for different number of test phases.

In practice, the need of the proposed filter is justified as the angular resolution of the C-BPS phase estimator (β) is significantly smaller than the resolution of the digital signal processor used to perform the algorithm. As an example, 32 and 64 possible test phase values or less (equivalent to <5 and <6 resolution bits, respectively) are recommended for CPR in the C-BPS for 16QAM and 64QAM respectively which, in a practical implementation of the algorithm, might be much lesser [2–11]. However, current technologies on ADC/DAC integrated in the ASICs as part of modern transceivers are shown to be able to achieve 8 bits of resolution [13]. Thus, being the number of employed test phases in the C-BPS CPR the limiting factor in terms of resolution. This, in practice, allows for a potential mitigation of the quantization noise as the C-BPS process provides a phase noise estimator with a lower resolution (<32 or <64 values for 16QAM and 64QAM respectively) than the resolution of the DSP ASIC’s processor employed to physically perform the algorithm (~8 bits) [13].

It is important to note the difference between the proposed angular quantization noise filter in the F-BPS and the C-BPS block filter. The block filter is used to average the AWGN influence on the distance metric calculation, while the proposed angular quantization noise filter in the F-BPS scheme is employed to reduce the out-of-band angular quantization noise of the C-BPS phase estimator. In order to maintain an implementable low overall complexity of the proposed F-BPS, low pass filters with low complexity implementation (sliding average filter (SAF) without weighting coefficients) are used in this paper for both the C-BPS block filter and the additional proposed angular quantization noise filter of the F-BPS scheme. Optimization of both filters might further improve the performance, but at the cost of a larger implementation complexity and it is not the purpose of this paper. It is also noted that the proposed filter differs from the parabolic interpolation filter shown in [14] as the aim of this filter is to interpolate the error metric distance function to obtain a more accurate phase estimator. Instead, as mentioned earlier, the purpose of the proposed angular quantization noise filter in this paper is to mitigate the out-of-band-quantization noise by low pass filtering the C-BPS phase noise estimator. Although both filters might tackle similar problems, they are different in nature, have different implementation complexity, might perform differently, and the decision on which to implement corresponds to the ASIC designer.

3. Simulation Results

A 28-Gbaud coherent optical back-to-back transmission system is simulated in VPItransmissionMakerTM [15] to compare the performance of the proposed filtered BPS (F-BPS) scheme with that of the conventional BPS (C-BPS). A pseudorandom bit sequence is created and mapped to 16QAM and 64QAM to generate signals of 2^{17} symbols of length. The generated signals are modulated on a lightwave carrier and loaded with additive white Gaussian noise (AWGN) to emulate erbium-doped fiber amplifier noise. The signals are then band pass filtered to remove out-of-band noise and directly fed into the receiver in order to isolate phase impairments from other fiber transmission impairments. A digital signal processing (DSP) based demodulator performing different DSP routines, as later shown in Section 4, is then applied.

Figure 3 shows the OSNR sensitivity penalty versus the combined linewidth symbol duration product for 16QAM and 64QAM signals employing the proposed F-BPS scheme and the ordinary C-BPS scheme with a different number of test phases. For the C-BPS case, its block filter length was optimized to show the best performance for all the points in the curves in Figures 3 and 4. For the F-BPS case, in order to reduce the large amount of simulations to be carried out, the C-BPS block filter bandwidth and the proposed angular quantization noise LPF bandwidth were swept together, with the same value, in order to show the best performance for all the points in the curves in Figures 3 and 4. It can be observed that the proposed F-BPS scheme improves the phase noise tolerance of the C-BPS algorithm for both 16QAM and 64QAM constellations when employing the same number of test phases. The relative performance improvement of the F-BPS scheme compared to C-BPS increases for low values of β test phases where the quantization noise is more prominent. For 16QAM, the C-BPS performance (@ 1 dB of OSNR penalty) employing 32 test phases can be achieved with the proposed F-BPS with only nine test phases. For 64QAM, the corresponding numbers are 12 test phases for F-BPS compared with 64 test phases for C-BPS. As observed in Figure 3, angular quantization noise causes large performance degradation in the C-BPS when the number of employed test phases are reduced from 32 to 9 for 16QAM and from 64 to 12 for 64QAM. Figure 4 illustrates the tolerable linewidth symbol duration product versus the number of β test phases of the F-BPS and C-BPS schemes for 16QAM and 64QAM. The results show the achievable phase noise tolerance for 1dB OSNR penalty at the BER FEC limits of 3.8×10^{-3} for 16QAM and 2×10^{-2} for 64QAM. For 16-QAM, a ~16% phase noise tolerance increase is observed for the F-BPS compared to C-BPS, when using 32 test phases in both schemes. For 64QAM, employing 64 test phases, a ~31% increase of phase noise tolerance is achieved with the proposed F-BPS scheme. It is noted that the complexity of the C-BPS algorithm is directly related to the number of employed test phases and its filter block length [16]. The authors have observed that, for the same linewidth levels, similar filter block lengths were required for both the C-BPS and the F-BPS cases even when employing different numbers of test phases. Hence, for 16QAM, a ~72% implementation complexity reduction can be achieved with the F-BPS ($\beta = 9$) compared to C-BPS ($\beta = 32$), while maintaining the same phase noise tolerance level. The complexity reduction is even larger for 64QAM where the reduction from $\beta = 64$ test phases for C-BPS to only $\beta \sim 12$ test phases leads to a 81% reduction of complexity without sacrificing performance. The complexity of the sliding average filter for quantization noise mitigation is negligible compared to that of the required computations for each extra test phase.

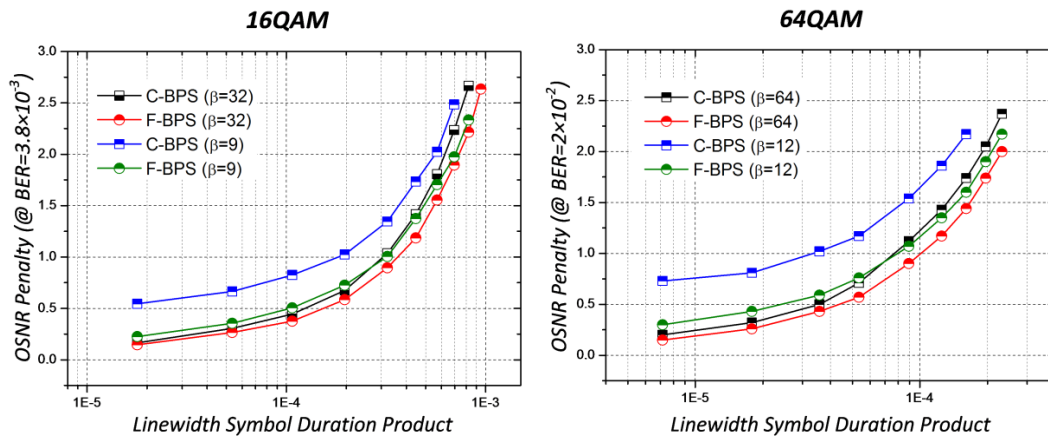


Figure 3. OSNR sensitivity penalty versus combined linewidth symbol duration product comparative between the proposed F-BPS and C-BPS for 16QAM and 64QAM employing different number of test phases at BER levels of 3.8×10^{-3} and 2×10^{-2} , respectively.

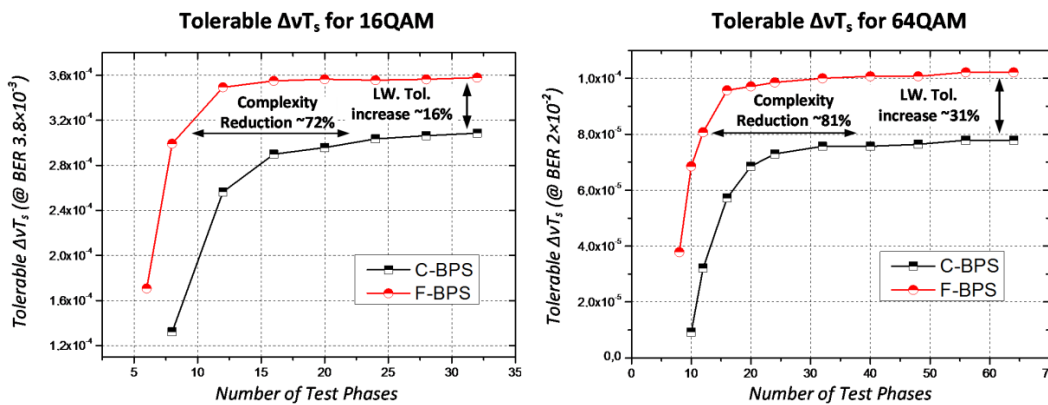


Figure 4. Tolerable combined linewidth symbol duration product comparative between the proposed F-BPS and C-BPS for 16QAM and 64QAM employing different number of test phases at BER levels of 3.8×10^{-3} and 2×10^{-2} , respectively, and for 1 dB OSNR penalty.

4. Experimental Setup and Results Validation

The experimental setup for the validation of the proposed F-BPS scheme is shown in Figure 5. The transmitter consists of two synchronized 50 GSa/s arbitrary waveform generators (AWG), an optical IQ modulator, and an external cavity laser (ECL) with less than 100 kHz linewidth. A pseudo-random bit sequence (PRBS15) is mapped to a 28-Gbaud 64QAM signal followed by Nyquist pulse shaping with a 0.15 roll off factor. The sequence is then re-sampled to match the sampling rate of the AWGs. A number of phase noise sequences are generated in order to emulate the phase noise of a semiconductor laser with different linewidths [17,18]. The generated phase noise sequences are then multiplied with the resampled signal and its I and Q components are loaded into each of the AWGs. The electrical output of the synchronized AWGs is fed into an optical IQ modulator which linearly modulates the incoming electrical signal onto the transmitting ECL. The 28-Gbaud 64QAM output of the IQ modulator is then amplified using an erbium doped amplifier (EDFA). An optical signal to noise ratio (OSNR) adjusting module consisting of an optical attenuator and an EDFA with constant output power is used to adjust the OSNR of the signal. The 64QAM signal is then fed in the receiver consisting of a balanced coherent receiver front end, an 80 GSa/s and 33 GHz bandwidth digital sampling oscilloscope (DSO), and an integrated LO laser with <100 kHz linewidth. Data demodulation is performed offline using DSP routines where the proposed F-BPS and C-BPS CPR schemes are applied for their performance comparison.

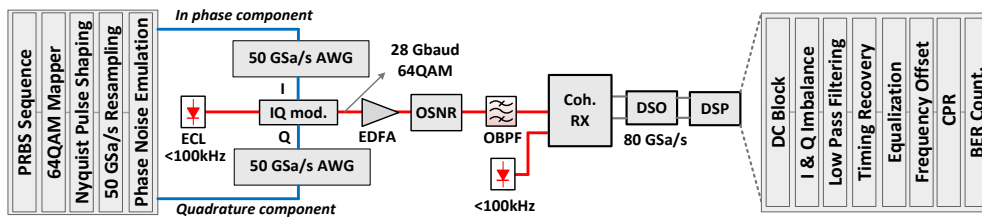


Figure 5. Experimental setup. AWG: Arbitrary waveform generator. EDFA: Erbium doped fiber amplifier. OBPF: Optical band pass filter. DSO: Digital signal oscilloscope. DSP: Digital signal processing.

Figure 6 shows the experimental performance validation of the proposed F-BPS and its comparison with the C-BPS algorithm in a 28-Gbaud 64QAM. Figure 6a shows the BER against the number of test phases at 31.8 dB of OSNR for three different emulated linewidths for the F-BPS and C-BPS schemes. For the C-BPS case, its block filter length was optimized to show the best performance for all points in the curves. For the F-BPS case, the C-BPS block filter length and the proposed angular quantization noise filter length were swept together, with the same value, to obtain the best performance for all the points in the curves. It is observed that the proposed filtering operation provides a phase noise tolerance improvement for all the three emulated linewidth cases compared to the C-BPS algorithm. It is also observed that the relative phase noise tolerance improvement increases for higher values of emulated linewidth. A significantly lower number of test phases for the F-BPS case is shown to be sufficient to achieve the C-BPS algorithm performance. Hence, showing a potential low complexity implementation of the algorithm as similar filter block lengths was required when optimizing the C-BPS and the F-BPS filter block lengths, for the same emulated linewidth cases, even when employing different number of test phases. Figure 6b illustrates the BER against OSNR curves for the proposed F-BPS ($\beta = 16$) and C-BPS ($\beta = 16, 64$) schemes for three different emulated linewidth levels. It is observed that similar or improved performance is achieved with the proposed F-BPS ($\beta = 16$) compared to that of the C-BPS ($\beta = 64$). If the same low number of test phases ($\beta = 16$) is used, a drastic performance improvement is achieved with the proposed F-BPS scheme. Figure 7 illustrates the improvement in the constellation diagram for 64QAM achieved by the F-BPS scheme (Figure 7b), using the proposed F-BPS for angular quantization noise mitigation, as compared to the unfiltered C-BPS algorithm (Figure 7a), both employing eight test phases ($\beta = 8$). In this case, the BER is halved when employing the proposed F-BPS solution. Figure 7c depicts, in frequency domain, the angular quantization noise of the phase estimator before (C-BPS) and after (F-BPS) the angular quantization noise low pass filter in the F-BPS for different numbers of test phases, illustrating the quantization noise mitigation.

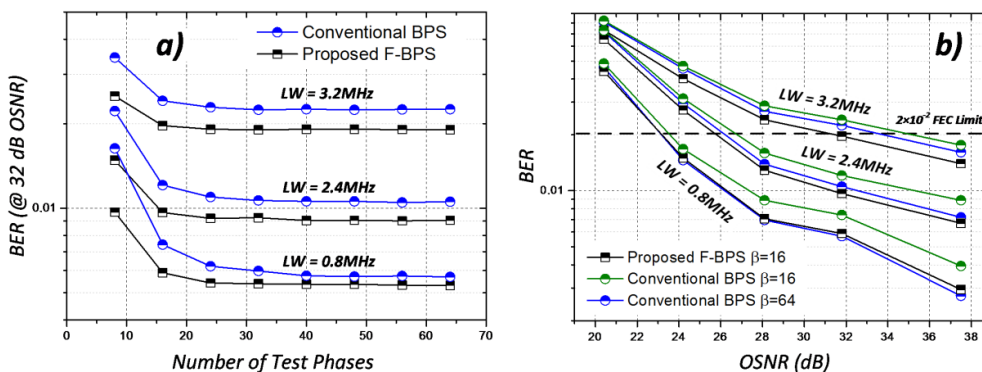


Figure 6. (a) Experimental BER versus number of test phases comparative between F-BPS and C-BPS for a 28-Gbaud 64QAM at different linewidth levels; (b) Experimental BER versus OSNR comparative between the F-BPS and C-BPS schemes for a 28-Gbaud 64 QAM at different linewidth levels.

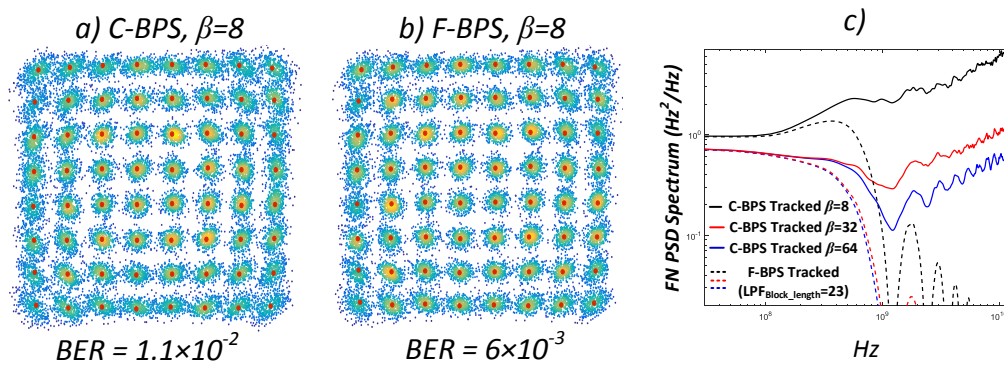


Figure 7. (a) 64QAM recovered constellation employing the C-BPS algorithm for CPR with eight test phases at 0.8 MHz of linewidth and 37.5 dB of OSNR; (b) 64QAM recovered constellation employing the proposed F-BPS algorithm for CPR with eight test phases at 0.8 MHz of linewidth and 37.5 dB of OSNR; (c) Frequency noise spectrum of different tracked phases by the C-BPS and the F-BPS.

5. Conclusions

The inherent discrete phase search nature of the conventional BPS (C-BPS) algorithm is shown to introduce quantization noise in its phase noise estimator which limits its phase noise tolerance and implementation complexity. A new CPR scheme, F-BPS, is proposed to mitigate the angular quantization noise of the C-BPS by using a LPF operation performed on the C-BPS phase noise estimator. The performance of the F-BPS scheme is evaluated both in simulations and experimentally for 16QAM and 64QAM signals to corroborate a significant phase noise tolerance increase. Results also show the possibility of drastically reducing the complexity implementation of the proposed CPR scheme as only a small number of test phases are required to achieve the same phase noise tolerance as for the C-BPS case.

Acknowledgments: This work was supported by EU project ICONE, gr. #608099, GRIFFON, gr. #324391, Vetenskapsrådet PHASE, gr. #2016-04510 and Swedish SRA ICT-TNG program. The equipment was funded by Knut and Alice Wallenberg foundation.

Author Contributions: J.R.N., A.K., and X.P., proposed the concept. J.R.N., A.K., X.P., O.O., A.U., and R.S., initiated the study. J.R.N. and A.K., carried out the simulations. J.R.N., A.K., X.P., O.O., and A.U. conducted the experimental analysis. R.S., S.P., and G.J. guided the studies. J.R.N., A.K., X.P., O.O., A.U., R.S., S.P., and G.J. participated in writing the manuscript.

Conflicts of Interest: The authors declare no conflict of interest.

References

- Viterbi, A. Nonlinear estimation of PSK-modulated carrier phase with application to burst digital transmission. *IEEE Trans. Inf. Theory* **1983**, *29*, 543–551. [[CrossRef](#)]
- Pfau, T.; Hoffman, S.; Noé, R. Hardware-efficient coherent digital receiver concept with feed forward carrier recovery for m-QAM constellations. *J. Lightwave Technol.* **2009**, *27*, 989–999. [[CrossRef](#)]
- Bilal, S.M.; Bosco, G.; Cheng, J.; Lau, A.P.T.; Lu, C. Carrier Phase Estimation through the Rotation Algorithm for 64-QAM Optical Systems. *J. Lightwave Technol.* **2015**, *33*, 1766–1773. [[CrossRef](#)]
- Zhang, F.; Wu, J.; Li, Y.; Xu, K.; Lin, J. Multi-stage feed-forward optical carrier phase estimation based on QPSK partitioning for 64-QAM signals. *Opt. Int. J. Light Electron. Opt.* **2013**, *124*, 2557–2560. [[CrossRef](#)]
- Bilal, S.M.; Fludger, C.R.S.; Curri, V.; Bosco, G. Multistage carrier phase estimation algorithms for phase noise mitigation in 64-quadrature amplitude modulation optical systems. *J. Lightwave Technol.* **2014**, *32*, 2973–2980. [[CrossRef](#)]
- Su, X.; Xi, L.; Tang, X.; Zhang, Z.; Bai, S.; Zhang, W.; Zhang, X. A Multistage CPE Scheme Based on Crossed Constellation Transformation for M-QAM. *Photon. Technol. Lett.* **2015**, *27*, 77–80.

7. Xiang, M.; Fu, S.; Deng, L.; Tang, M.; Shum, P.; Liu, D. Low-complexity feed-forward carrier phase estimation for M-ary QAM based on phase search acceleration by quadratic approximation. *Opt. Express* **2015**, *23*, 19142–19153. [[CrossRef](#)] [[PubMed](#)]
8. Zhong, K.P.; Ke, J.H.; Gao, Y.; Cartledge, J.C. Linewidth-Tolerant and Low-Complexity Two-Stage Carrier Phase Estimation Based on Modified QPSK Partitioning for Dual-Polarization 16-QAM Systems. *J. Lightwave Technol.* **2013**, *31*, 50–57. [[CrossRef](#)]
9. Li, J.; Li, L.; Tao, Z.; Hoshida, T.; Rasmussen, J.C. Laser-linewidth-tolerant feed-forward carrier phase estimator with reduced complexity for QAM. *J. Lightwave Technol.* **2011**, *29*, 2358–2364. [[CrossRef](#)]
10. Zhou, X. An improved feed-forward carrier recovery algorithm for coherent receivers with m-QAM modulation format. *Photon. Technol. Lett.* **2010**, *22*, 1051–1053. [[CrossRef](#)]
11. Zhou, X.; Lu, C.; Lau, A.P.T.; Long, K. Low-complexity carrier phase recovery for square m-QAM based on S-BPS algorithm. *Photon. Technol. Lett.* **2014**, *26*, 1863–1866. [[CrossRef](#)]
12. Navarro, J.R.; Kakkar, A.; Schatz, R.; Pang, X.; Ozolins, O.; Nordwall, F.; Louchet, H.; Popov, S.; Jacobsen, G. High performance and low complexity carrier phase recovery schemes for 64-QAM coherent optical systems. In Proceedings of the Optical Fiber Communication Conference and Exhibition (OFC), Los Angeles, CA, USA, 19–23 March 2017.
13. Bower, P.; Dedic, I. High speed converters and DSP for 100G and beyond. *Opt. Fiber Technol.* **2011**, *17*, 464–471. [[CrossRef](#)]
14. Sun, H.; Wu, K.T.; Thomson, S.; Wu, Y. Novel 16QAM carrier recovery based on blind phase search. In Proceedings of the European Conference and Exhibition on Optical Communications (ECOC), Cannes, France, 22–24 September 2014.
15. VPIphotonics GmbH, Carnotstrasse 6, DE-10587 Berlin, Germany. Available online: <http://www.vpiphotonics.com> (accessed on 22 May 2017).
16. Navarro, J.R.; Kakkar, A.; Pang, X.; Ozolins, O.; Schatz, R.; Olmedo, M.I.; Jacobsen, G.; Popov, S. Carrier Phase Recovery Algorithms for Coherent Optical Circular mQAM Systems. *J. Lightwave Technol.* **2016**, *34*, 2717–2723. [[CrossRef](#)]
17. Kikuchi, K. Characterization of semiconductor-laser phase noise and estimation of bit-error rate performance with low-speed offline digital coherent receivers. *Opt. Express* **2012**, *20*, 5291–5302. [[CrossRef](#)] [[PubMed](#)]
18. Zan, Z.; Lowery, A.J. Experimental demonstration of a flexible and stable semiconductor laser linewidth emulator. *Opt. Express* **2010**, *18*, 13880–13885. [[CrossRef](#)] [[PubMed](#)]



© 2017 by the authors. Licensee MDPI, Basel, Switzerland. This article is an open access article distributed under the terms and conditions of the Creative Commons Attribution (CC BY) license (<http://creativecommons.org/licenses/by/4.0/>).